

Broadband UV-, VIS-, and IR-Radiometric, Photometric, Color, and Temperature Measurements

Broadband UV-, VIS-, and IR-Radiometric, Photometric, Color, and Temperature Measurements

By

George P. Eppeldauer

**Cambridge
Scholars
Publishing**



Broadband UV-, VIS-, and IR-Radiometric, Photometric, Color,
and Temperature Measurements

By George P. Eppeldauer

This book first published 2021

Cambridge Scholars Publishing

Lady Stephenson Library, Newcastle upon Tyne, NE6 2PA, UK

British Library Cataloguing in Publication Data

A catalogue record for this book is available from the British Library

Copyright © 2021 by George P. Eppeldauer

All rights for this book reserved. No part of this book may be reproduced, stored in a retrieval system, or transmitted, in any form or by any means, electronic, mechanical, photocopying, recording or otherwise, without the prior permission of the copyright owner.

ISBN (10): 1-5275-6759-1

ISBN (13): 978-1-5275-6759-7

TABLE OF CONTENTS

Preface	ix
1. Introduction	1
2. Spectrally integrated (broadband) responsivity calibrations.....	3
2.1 Detector-based photometry	4
2.1.1 Illuminance reference scales.....	5
2.1.1.1 Illuminance measuring transfer-standards.....	8
2.1.1.2 Illuminance meter working standards	11
2.1.1.3 Photometer calibrations	15
2.1.1.4 Illuminance responsivity	20
2.1.1.5 Test photometers	22
2.1.2 Spectral mismatch correction.....	23
2.1.3 $V(\lambda)$ mismatch index f'_1	25
2.1.4 Candela realization.....	26
2.1.4.1 The illuminance unit	27
2.1.4.2 Luminous intensity	29
2.2 Tristimulus colorimeters	29
2.2.1 Characteristics of tristimulus meters	30
2.2.2 Responsivities of realized tristimulus meters	32
2.2.3 Integrated responsivity calibration of tristimulus meters	35
2.2.4 Validation and recalibration of tristimulus meters	39
2.2.5 Matrix corrections for solid-state light-source measurements.....	40
2.3 Tunable output LED source for scale transfer.....	43
2.4 Absolute calibration of digital imaging systems (cameras)....	47
2.5 Detector-based temperature calibrations	55
2.5.1 Radiation thermometry	56
2.5.2 Radiance responsivity calibrations.....	58
2.5.3 Radiation thermometer design and characterization....	60
2.5.4 Radiance responsivity of radiation thermometer.....	61
2.5.5 Determination of detector-based temperatures	62
2.5.6 Radiation thermometer linearity test	63

2.5.7 Determination of the Ag- and Au-freezing temperatures	64
2.5.8 Comparison of ITS-90 and thermodynamic temperatures	65
2.5.9 New designs for radiation thermometers	66
2.5.9.1 Design improvements of thermal IR radiation thermometers	68
2.5.9.1.1 Experimental setup	70
2.5.9.1.2 Infrared detector selection	71
2.5.9.1.3 Optical design	75
2.5.9.2 Radiation thermometer calibration	76
2.5.9.3 Radiation thermometer characterizations	79
2.5.9.3.1 Temporal stability	80
2.5.9.3.2 Noise equivalent temperatures	84
2.5.9.3.3 Size of source effect	86
2.5.9.4 ART temperature measurement uncertainties	87
2.5.9.5 Discussion and conclusions of the ART development.....	88
2.5.10 Development of a future temperature scale	89
3. Broadband LED radiometric measurements	95
3.1 CIE recommended UV measurements.....	95
3.2 Procedure for uniform UV measurements.....	97
3.2.1 Problems of CIE-standard rectangular-shape UV-meter responses	99
3.2.2 UV detectors selection	102
3.2.3 UV irradiance meters selection	102
3.2.4 Spectral modelling of LED-365 measurements	105
3.2.5 LED-365 irradiance source development and selection	108
3.2.5.1 LED irradiance source calibration against FEL-lamp standard	112
3.2.6 Integrated irradiance measurement methods	115
3.2.6.1 Non-flat response method using LED-365 standard	116
3.2.6.2 Flat-response UV-meter-based calibrations without a source standard.....	120
3.2.6.3 Average-responsivity standard.....	121
3.2.6.4 Use of filtered-Si detector of flat-response.....	121
3.2.7 Reference UV-365 filter-radiometers	124
3.2.8 Flat-response pyroelectric UV-to-SWIR radiometer ...	127

3.2.9 Reflectance-based in-situ pyroelectric response determination.....	130
3.2.10 Flat-response pyroelectric radiometers measure integrated irradiance of UV LEDs.....	137
3.2.10.1 LED-365 irradiance measurement using pyroelectric detector standard.....	146
3.2.10.2 Validation of pyroelectric detector measured integrated irradiance	148
3.2.10.3 Flat LiNbO ₃ pyroelectric detector to measure high power LEDs.....	150
3.2.11. Integrated irradiance responsivity of field UV meters	152
3.3 Suggestion for a portable UV-VIS-IR integrated irradiance meter	153
3.4 Radiance transfer to VIS and IR LEDs.....	156
3.4.1 Night Vision (NV) Goggle gain calibrations	157
3.4.2 Detector-based reference radiance realization	159
3.4.3 Radiance transfer using flat-response NV Transfer Radiometers (TR).....	162
3.4.4 Traceability of the NV-TRs	164
3.4.5 Reference irradiance meter of NV-TR Calibrations	164
3.4.6 First generation NV radiometer transfer standard.....	166
3.4.7 Second generation NV transfer standard radiometers	171
3.4.8 SI traceable radiance and luminance levels of NV Goggle test-sets	176
4. SI traceable calibration of photocurrents.....	182
4.1 DC mode transimpedance-type reference current-to-voltage converters.....	183
4.1.1 Feedback resistor selections.....	186
4.1.2 Reference current-to-voltage converter design.....	188
4.1.3 Feedback resistor calibrations	190
4.1.4 DC input current and signal-gain calibrations	191
4.1.5 Inter-comparison, validation, and measurement uncertainties.....	194
4.1.6 Nonlinearity test of DC current sources and meters	202
4.2 AC transimpedance-type current-to-voltage converters.....	206
4.2.1 Extension of the DC current-to-voltage conversion to AC	206

4.3 Input-current and gain calibration of charge measuring (switched) integrators	211
5. Uncertainties of spectrally integrated (broadband) radiant power measurements	214
References	217

PREFACE

Improved detector technology in the past two decades opened a new era in the field of optical radiation measurements. An increased number of calibration and measurement facilities and procedures could be developed with lower measurement uncertainties using the newly developed detector/radiometer standards instead of traditionally applied source standards (blackbodies and lamps). Shrinking of the traditional source-based calibrations and the large increase of optical detector-based calibrations motivated the writing of this book series.

The book series is a comprehensive description of optical detector based radiometric practices. Instead of giving the traditional lexical-type tutorial information, a research-based material is systematically organized and described. The large number of examples cover modern detector applications in the field of radiometry, photometry, colorimetry, and radiation temperature measurements. All the discussed devices and applications have been implemented, realized, tested, verified, and evaluated. These applications are described to obtain uniform results with low measurement uncertainties. They are described with enough details to successfully repeat them by the readers/users. The applications and evaluations follow the recommendations of international standardization. The described subjects are detailed and distributed in five volumes.

Properties of radiometric quality detectors, their use and selection for optical radiometers, design considerations of radiometers and detector-based standards, description of spectral and broadband detector-based calibrations and measurements using modern setups based on the new radiometer standards are described for practicing scientists, engineers, and technicians.

The book series includes many hundreds of designs, drawings, measurement schemes, a large number of detector-based measurement and calibration setups, measurement equations and results, calibration-transfer and measurement methods/procedures all tested in practical applications.

In addition to reference level detector/radiometer calibrations, measurement of radiometric quantities used in practice (secondary laboratory and field applications), are discussed. Such quantities are radiant power, irradiance, and radiance. Measurement of spectral and broadband (integrated) quantities are discussed from 200 nm in the ultraviolet to 30 μm in the infrared.

All discussed calibrations and measurements are traceable to the System International (SI) units through National Measurement Institutes (NMIs) and/or the discussed intrinsic detector standards.

Linear and traceable measurement of detector output signals, including DC and AC photocurrent (sub-scale) and voltage measurements, detector-amplifier gain-calibrations, and gain-linearity tests are discussed in detail.

Uncertainty determination/calculation methods of detector-based measurements are described. It is a general rule for the discussed large number of design and application examples, to keep the calibration/measurement uncertainties low.

The author thanks all the colleagues listed in the references at the end of each volume for their help and contribution to perform the discussed large number of measurements and evaluations.

Dr. George P Eppeldauer, author



1. INTRODUCTION

In most practical/field applications broadband measurements are used where the spectral product of the source distribution and the meter's spectral responsivity is measured. While in photometry, the standardized spectral response function of the meter covers only the visible interval, measurements outside the visible spectral interval (e.g. ultraviolet or infrared) require different standards. Using a traditional detector- or source-standard, the differences in the spectral distributions of test sources (like LEDs) and in the spectral responsivities of the source measuring detectors produce non-uniform broadband measurements with large errors. To perform uniform broadband measurements, a signal measurement procedure had to be developed and introduced. This new procedure, described here in detail, should be introduced as an international standard to solve long-existing measurement uncertainty problems, especially in the ultraviolet range. The new procedure can be applied for sources (like LEDs) and also for detectors and radiometers. A simple version of the procedure can be utilized by using a flat-response pyroelectric detector (similarly to a lux meter) to measure integrated irradiance, the radiometric equivalent of illuminance, from UV to IR. The calibration procedure of the optical radiation measuring detector-preamplifier (radiometer) is also discussed. The book is to guide the optical radiation measurement community, researchers, manufacturers, calibration laboratories, students, and practicing engineers to switch from single-standard based broadband calibrations to signal-measurement-procedure based broadband calibrations to obtain uniform measurement results with low uncertainty.

Utilizing the new generation optical detectors and radiometers and using the signal-measurement-based broadband radiometric measurement procedure makes it possible to determine the integrated irradiance from different UV and IR sources (like LEDs and IR background radiation), and to make radiance transfer to VIS and IR LEDs e.g., to measure night vision goggle (NVG) gains in NVG calibration test-sets. Improving the uncertainty of DC photocurrent calibrations to the sub 0.01 % ($k=2$) level, and AC photocurrent calibrations to the 0.04 % ($k=2$) level made it possible

to decrease uncertainties in SI traceable radiometric, photometric, tristimulus-color, and radiation thermometry measurements.

2. SPECTRALLY INTEGRATED (BROADBAND) RESPONSIVITY CALIBRATIONS

Improvements in detector technology over the past two decades have opened a new era in the field of radiometric and photometric calibrations. Lower measurement uncertainties can be achieved with modern detector standards than with traditionally used source standards.

Traditionally, radiometric, photometric, and color calibrations came from the source side. Color temperature, irradiance, and luminous intensity standard lamps were calibrated against black-body radiators through several derivation steps. Because of the multiple-step calibration procedures, and the significant change of source characteristics during and between calibrations, long term reproducibility of close to 1 % ($k=2$) could happen in addition to the close to 1% ($k=2$) spectral irradiance uncertainty (with respect to SI units) on the test irradiance lamps in the visible range [1]. Traditionally, color temperature scales are based on spectral irradiance scale with the additional application of the CIE standardized weighting functions [2]. Color temperature is a light source parameter related to spectral quality (relative spectral power or irradiance distribution).

Recently, fundamental photometric and radiometric scales have been realized and maintained using detector-based standards [3-5]. The reference spectral responsivity scales discussed in Volume 4 (Detector-Based Reference Calibrations for Electro-Optical Instruments) of this book series are utilized here to perform broadband photometric and radiometric calibrations and measurements in practical (field) applications with low uncertainties. In broadband measurements, the spectral product of the source distribution and the meter's spectral responsivity is measured. In photometry, the spectral response of the meter is standardized. The CIE standardized spectral response function (see below) covers only the visible wavelength interval. Measurements outside of the visible

range (e.g. ultraviolet or infrared) require different standards. SI traceable broadband measurements and calibrations from the UV to the IR, using modern optical detector/radiometer standards, are discussed here.

2.1. Detector-based photometry

Photometry is a subset of optical radiometry where broad-band visible radiation (light) is measured with detectors of standardized spectral responsivity. In 2019 the International System of Units (SI) was redefined. The definitions of the SI units are established in terms of a set of seven defining constants. The complete system of units can be derived from the fixed values of these defining constants expressed in the units of the SI [6]. These constants were chosen by taking into account the previous definition of the SI which was based on seven base units. The photometric base quantity is the luminous intensity with the candela base unit. The candela, symbol cd, is the SI unit of luminous intensity in a given direction. It is defined by taking the fixed numerical value of the luminous efficacy of monochromatic radiation of frequency $540 \cdot 10^{12}$ Hz, K_{cd} , to be 683 when expressed in the unit lm W^{-1} , which is equal to cd sr W^{-1} , or $\text{cd sr kg}^{-1} \text{m}^{-2} \text{s}^3$, where the kilogram, meter and second are defined in terms of h , c , and $\Delta\nu_{Cs}$. The exact expression for the candela in terms of the defining constants [6] is

$$1 \text{ cd} = 2.614830 \times 10^{10} (\Delta\nu_{Cs})^2 h K_{cd}$$

The effect of this new definition is that one candela is the luminous intensity in a given direction of a source that emits monochromatic radiation of frequency $540 \cdot 10^{12}$ Hz and has a radiant intensity in that direction of $(1/683) \text{ W/sr}$.

According to the definition, photometry is directly related to radiometry. The definition gives the conversion factor $(1/683)$ at one wavelength between photometric (luminous) and radiometric (radiant) intensity. The definition means that 683 lumen (lumen=candela * steradian) is equal to 1 W at $540 \cdot 10^{12}$ Hz, where lumen is the unit of luminous flux, the photometric equivalent of radiant power. In photometry, the radiant power of different wavelengths is weighted according to the spectral sensitivity of the human visual system. The weighting function for photopic vision (at high luminous flux levels) is $V(\lambda)$,

which peaks at a value of 1 at 555 nm [4], the corresponding wavelength of the 540×10^{12} Hz frequency in the candela definition.

The above definition gave a new possibility for realizing photometric scales using detector standards. According to the candela redefinition a photometric detector of known relative $V(\lambda)$ spectral response (photometer) requires an absolute response calibration at 555 nm only, to tie its photometric spectral response to a radiometric (absolute) detector response at 555 nm.

2.1.1. Illuminance reference scales

Not only national laboratories [7, 8], but also small research facilities [9] have taken advantage of these possibilities. It was common that either absolute radiometers or spectrally calibrated silicon photodiodes were equipped with photopic correcting filters. Different kinds of absolute radiometers were used: a cryogenic electrical substitution radiometer with silicon photodiode transfer standards [7], electrically calibrated thermal detectors [8], and self-calibrated silicon photodiodes [10].

Change of the source standards to detector standards in the photometric and color scale realizations resulted in significant improvements in the scale uncertainties at the National Institute of Standards and Technology (NIST). In a photometric unit realization, typically, the major source of uncertainty is the spectral responsivity determination of the photometers. At NIST, the Spectral Comparator Facility (SCF) [11] that utilizes a monochromator and a lamp was used to measure the spectral responsivity of photometers.

A calibration facility for Spectral Irradiance and Radiance Responsivity Calibrations using Uniform Sources (SIRCUS) has been developed at NIST later [12] to overcome the limitations of the SCF, in particular for calibrating irradiance and radiance meters. The facility introduces the output from tunable lasers into integrating spheres, producing a monochromatic, high-power uniform source. Earlier, the responsivity scale was transferred from the NIST High-Accuracy Cryogenic Radiometer [13] and maintained on irradiance standard 6-element transmission trap detectors. Their spectral power responsivity was determined using a cryogenic electrical substitution radiometer, and their irradiance responsivity was derived by placing a calibrated aperture at the input plane. The SIRCUS facility has several advantages

over conventional lamp-monochromator systems to realize photometric and colorimetric scales. It provides high-power, low wavelength uncertainty, and the ability to produce a monochromatic Lambertian radiation that enables calibration of instruments directly for irradiance or radiance responsivity.

The overall relative combined expanded ($k=2$) uncertainty for the NIST illuminance unit realization using the SCF was 0.39 % [11]. There are several components in the uncertainty budget related to the determination of the photometer spectral responsivity in the SCF. These uncertainty components were significantly reduced by realizing the illuminance scale on the SIRCUS facility.

The standard uncertainty in the spectral responsivity scale can be reduced from 0.11 % (measured on the SCF) to 0.075 % due to the reduction of transfer steps from the absolute cryogenic radiometer. The CIE spectral luminous efficiency, $V(\lambda)$, is a strong function of wavelength. The SIRCUS wavelength scale, with uncertainties reduced to 0.001 nm from the SCF's wavelength uncertainty of 0.1 nm, can reduce the relative standard uncertainty for this component from 0.04 % to less than 0.001 %. A significant set of uncertainty components results from the geometry of the SCF output beam. The SCF uses $f/9$ optics to focus the light to a 1 mm spot that is used to calibrate the photometers. The photometers are used in a far field condition. SIRCUS can calibrate photometers in a geometrical configuration identical to the application geometry. In addition, since SIRCUS calibrates the detector in irradiance mode instead of power mode, the uncertainty of the aperture area and the uncertainty due to the non-uniform spatial response of the photometer will be eliminated. The combined uncertainty from these components related to measurement geometry can be reduced from 0.12 % to less than 0.01 %. The overall relative expanded uncertainty ($k=2$) for the NIST illuminance unit realization could be reduced to 0.24 %, a 40 % reduction in the uncertainty in the 2014 scale. The improved illuminance scale resulted in an overall relative expanded uncertainty of 0.27 % ($k=2$) for the NIST candela.

The NIST detector-based photometric scale [3] was based on the development of a group of eight illuminance meters. They contained the Commission Internationale de l'Eclairage (CIE) standardized $V(\lambda)$ matching filters equipped with temperature monitors and specially selected silicon photodiodes and photocurrent measuring

electronic circuits. These photometers still hold the photometric scale with a long-term illuminance responsivity change of less than 0.1 %. Working standard photometers with analog temperature control were also developed to disseminate the scale easier.

The NIST illuminance responsivity scales have been realized at two different calibration facilities. The scale, published in 1996, has a relative expanded uncertainty of 0.39 % ($k=2$). With the development of the Spectral Irradiance and Radiance Responsivity Calibrations with Uniform Sources (SIRCUS) facility [12], the spectral irradiance responsivity uncertainty could be lowered compared to the Spectral Comparator Facility (SCF) based scale. It was studied how to improve the uncertainty of the SCF based scale. In order to satisfy this goal, high quality transfer standard photometers have been developed. These transfer standards can be calibrated not only at the SCF, but also at the SIRCUS. At SIRCUS, stabilized tunable-lasers are coupled into integrating sphere sources producing uniform irradiance for the irradiance measuring reference trap detectors and the illuminance measuring photometers. As a result of the SIRCUS used calibration geometry, the uncertainty of the SIRCUS made spectral irradiance responsivity calibrations can be dominated by the 0.06 % ($k=2$) uncertainty of the reference Si trap-detector [14]. However, the old photometer standards, developed for the SCF-based scale realization, could not be calibrated at the SIRCUS because the remaining coherence at the sphere outputs caused large interference fringes. Development of the new transfer standards was needed to fix this problem. The SCF-based calibration had a longer scale derivation chain than the SIRCUS-based calibration since the transfer standard photometers were calibrated against the old photometer standards with substitution when both photometers measured the same illuminance of a 2856 K lamp. The difference of the SIRCUS and SCF determined illuminance responsivity measurements was 0.4 %. Though, this difference is within the reported uncertainties of the two different scale realizations of the two facilities, the goal was to decrease this difference and to obtain a better agreement between the two scales. In order to achieve this goal, the major uncertainty components of the two independent photometric scale realizations were analyzed, improved and then compared.

The main design issues and characteristics of the photometers and tristimulus colorimeters, the spectral responsivity calibrations, the

illuminance responsivity and color temperature scale-realizations and scale-validations, the related measurement issues and the improvements obtained with the matrix corrections are discussed below when different kinds of light sources are measured.

2.1.1.1. Illuminance measuring transfer-standards

The transfer standards were designed such that it is the uncertainty of the spectral irradiance responsivity calibrations that determines the photometric scale uncertainty and not limitations in the performance of the photometers themselves. New filter combinations have been designed with a minimum allowed thickness of 4.5 mm to avoid interference fringes. They are individually fabricated to closely match the responsivity of the silicon detector to the CIE $V(\lambda)$ function [4]. The filter combinations are in a filter wheel located between the common detector and aperture. The wheel temperature is controlled at 25 °C where the spectral mismatch errors were minimized.

Two types of transfer standard photometers were designed and built. The first type, as shown in Fig. 1, uses windowless silicon photodiodes in a tunnel trap configuration [14]. The front panel is removed for better illustration. A temperature-controlled filter-wheel was inserted and moved between the input aperture and the silicon tunnel-trap detector. The long-term stability of this photometer was regularly monitored to see if any responsivity changes happen due to either stain settlement on the filter surfaces or because the photodiodes are exposed to the ambient air. The stain from the front of the filters was removed yearly. Still, the illuminance responsivity decreased with 0.2 % from 2003 to 2007 and with another 0.1 % - 0.15 % to 2009. The change was close to 0.5 % at 400 nm and it gradually decreased and became negligibly small at 500 nm. In this tunnel-trap detector, light is not reflected back to the filters.

In the improved (newer) transfer standard, a single-element silicon photodiode is used which has a sealed wedged-window to avoid fringes. The picture of this transfer standard, (Model FIM #100 and #101), showing both the back and front-sides, is shown in Fig. 2. The front panels are removed for better illustration. The light tight box includes a filter-wheel. The filter position can be selected with the rotating knob located on the back side. The Y-channel is used as an absolute photometer. The photocurrent meter is attached to the side of the box. The current measuring electronics are matched to the

electronic characteristics of the photodiode for low-noise performance over a signal dynamic range of 12 decades. The uncertainty of the current-to-voltage conversion is less than 0.02 % ($k=2$).



Fig. 1. Filtered trap-detector based transfer standard photometer.

The detector is a large-area (1 cm x 1 cm) single-element silicon photodiode. The 0.5 ° wedge of the sealing window was needed to avoid interference fringes in the output signal of the photodiode. The spaces on the two sides of the temperature-controlled filter-wheel are small resulting in five orders of magnitude blocking in the near-IR even in overfilled mode. The less than 0.3 % peak-to-peak fringes of the Y-channel (as measured at the SIRCUS) before and after filtering the data are shown in Fig. 3. The filter combination was individually optimized to the CIE standard $V(\lambda)$ function. No responsivity degradation could be measured on this improved photometer between 2007 and 2009.



Fig. 2. Front and back pictures of two (single-element Si photodiode used) transfer-standard photo/colorimeters.

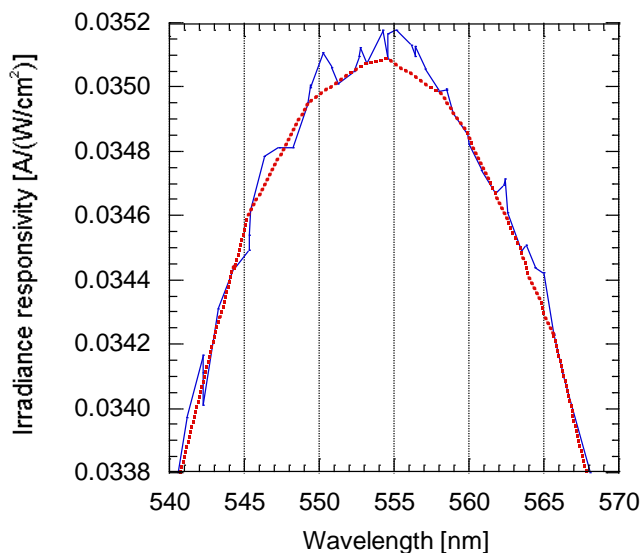


Fig. 3. Filtered fringes of the SIRCUS measured trap-photometer.

Also, the baffling inside of the trap-photometer was not efficient enough. Figure 4 shows that in overfilled mode (at SIRCUS), because of the internal reflections of the photometer, the Si trap detector (that peaks at 970 nm), measured a small portion of the incident light which did not go through the $V(\lambda)$ filter. In underfilled mode (at SCF), the stray and reflected light attenuation was two orders of magnitude better.

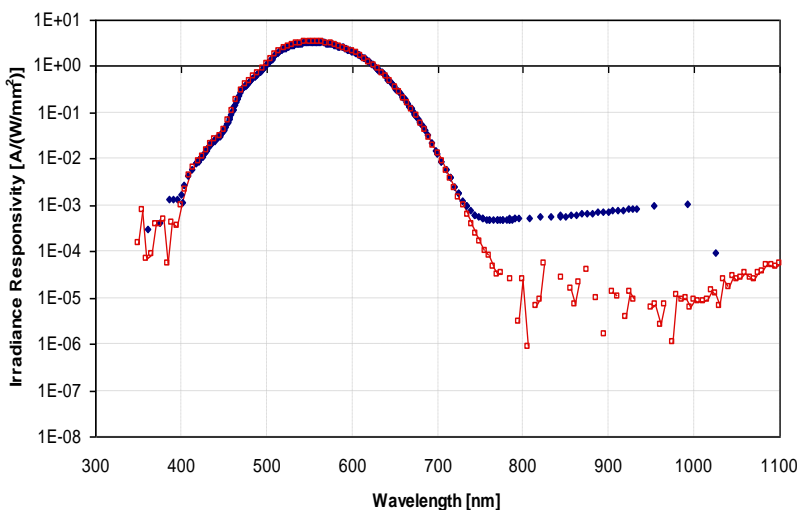


Fig. 4. SIRCUS (full-diamonds) and SCF (open squares) measured trap-photometer irradiance-responsivities including the unfiltered internal stray and reflected light.

2.1.1.2. Illuminance meter working standards

The illuminance responsivities of the working standard photometers have been determined yearly based on their spectral power responsivity measurements at the NIST SCF. Figure 5 shows the long-term changes of three working standards normalized to unity in 1991. Yearly scale realizations were made to determine the actual responsivities based on the SCF scale realizations. The line shows a 0.3 % maximum responsivity change for the group-average of photometers 4, 6, and 8. The front surfaces of the filters were not cleaned until 2006. The results show that the long-term stability of the individual photometers can be improved to ± 0.1 % if the front surfaces of the filters are cleaned on a regular basis.

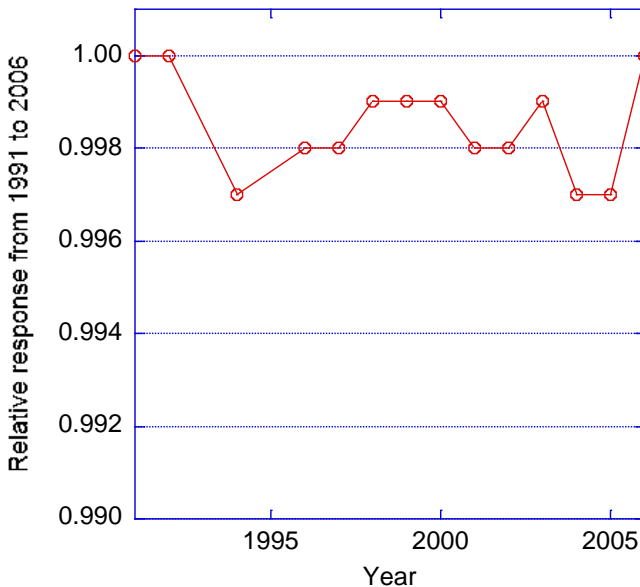


Fig. 5. Average 15-year changes of three photometer working standards. The photometers were cleaned only in 1991 and 2006.

Ten-year long changes of 0.02 % were reported on silicon photodiodes sealed with fused silica windows [15] used in these working standards. It can be concluded that change-free photometer standards can be made if the photometer head is sealed with a fused silica window. The stability of the working standards should be matched to the lower uncertainty of the SIRCUS-based scale to obtain an overall uncertainty improvement in the disseminated scale. A package design was applied for both the old and the new working standard photometers to obtain a uniform temperature distribution for the filter combination and the silicon photodiode. The steep short-wavelength slope of the $V(\lambda)$ curve acts like a thermometer. Also, the applied infrared-suppressed silicon photodiode has a significant temperature coefficient of responsivity at wavelengths longer than 630 nm. These two components are mounted in a metal housing. The uniform temperature is monitored in the existing (old) photometers [5] and stabilized in the new working standards. As shown in Fig. 6, the aperture, the filter combination (dotted), and the photodiode (hatched) are close to each other inside of a Copper pot.

While there is a small gap between the photodiode and the filter, the very thin aperture is mounted on the front surface of the filter to avoid inter-reflections. To simply cleaning the front surface of the filter, the aperture is fixed in a holder that can be easily removed and relocated into the same position using an asymmetric screw arrangement. A temperature sensor (in the lower left corner)) is plugged into the copper pot. A ring shape thermoelectric cooler is mounted to the bottom of the copper pot in the new working standards to keep the temperature constant, just above the ambient.

The field-of-view (FOV) of the illuminance meter depends on the diameter of the aperture and the photodiode active area. It is always kept small (in this case 11°) to reject ambient light as well as reflections and stray light from a test source. The base unit, as shown in Fig. 7, can be equipped with a mechanical mount (holder) at the front to attach an input optic (as shown by a sketch in Fig. 8) for luminance measurement. In a slightly different design, the filter can be removed and its temperature could be independently controlled from the temperature of the photodiode. The photocurrent meter is located inside of another cylindrical housing attached to the bottom of the base unit. The electronic characteristics of the current-to-voltage converter are matched to the high shunt resistance of the silicon photodiode to obtain low output-noise and wide signal range.

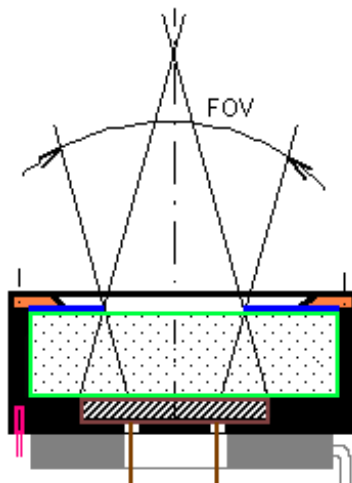


Fig. 6. Structure of a photometer package.

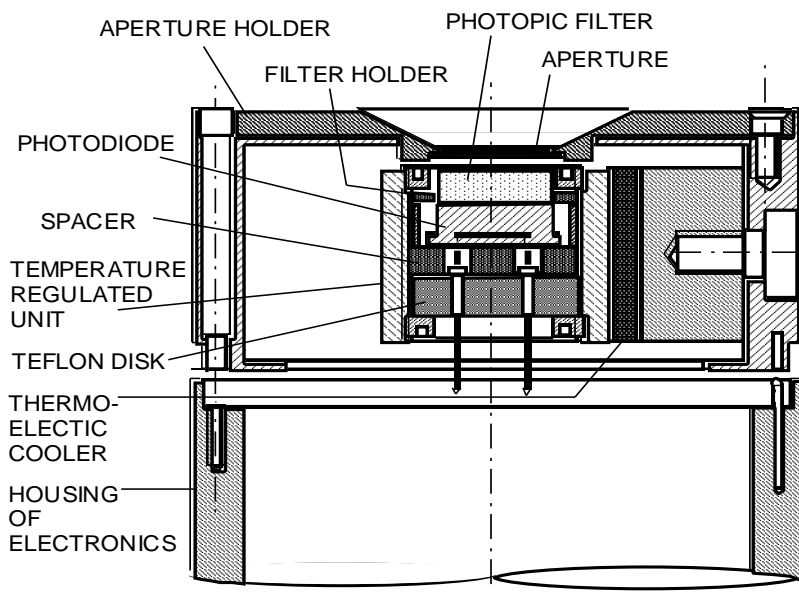


Fig. 7. Base unit of a photometer working standard.



photometers.

2.1.1.3. Photometer calibrations

While the SIRCUS facility can measure irradiance, the basic operational mode of the SCF facility is radiant power measurement. It was necessary to determine the aperture areas for both reference photometers. The aperture areas were determined from a raster-scan method at the SCF when the photopic filter was removed from the photodiode. The f/9 scanning beam did not cause multiple reflections between the aperture and the detector because of the 14 mm separation between them in the new reference photometers. The aperture areas were also determined from an irradiance-to-power responsivity ratio measurement at the SIRCUS. In this case, the irradiance responsivity was performed with a “point source”

geometry and the area determination was made against the known aperture area of the reference Si-trap detector of the SIRCUS (at one laser wavelength). The trap-detector aperture was calibrated at the NIST aperture-area calibration facility with 0.02 % ($k=2$) uncertainty [16]. The obtained aperture areas are shown in Table 1.

Table 1. Measured aperture areas of the F100 transfer-standard photometer.

	SIRCUS	SCF
Area [mm ²]	19.730	19.708

The difference between the SIRCUS and the SCF measured areas was 0.11 %. The relative expanded uncertainties of both methods were less than 0.08 % ($k=2$).

The 5 mm diameter aperture of the transfer standard photometers caused a beam clipping during the spectral power responsivity calibrations at the SCF. The 1.1 mm diameter monochromatic beam imaged to the aperture plane had some spatially scattered light (halo) around the aperture-hole which was clipped by the aperture itself. The halo was caused by imaging problems (degradation in the Aluminum mirrors). Because of the clipping, less flux was measured by the photometers than with the reference Si detector of the SCF. The loss caused by the beam clipping was measured using a 10 mm diameter silicon photodiode and a 5 mm diameter aperture (from the same batch as the photometer aperture). The aperture was in front of the detector during one spectral scan and then removed for the second measurement. Figure 9 shows the per-cent response difference obtained from the two measurements.

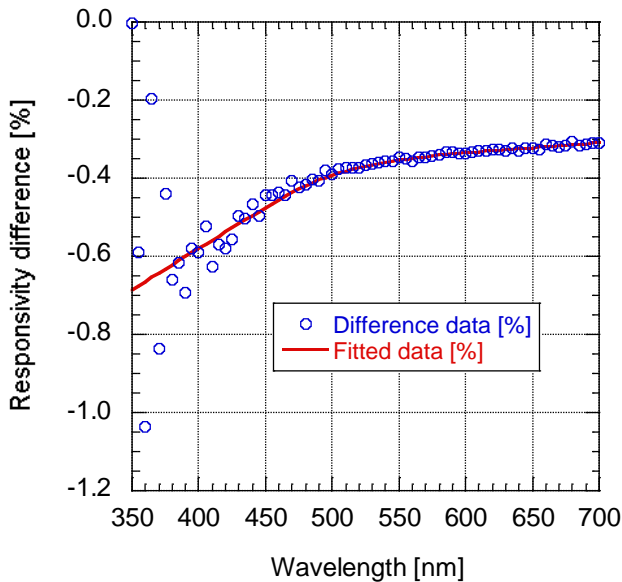


Fig. 9. Response difference of two SCF responsivity measurements made with and without a 5 mm aperture in front of a large Si photodiode.

The beam clipping was wavelength dependent. To decrease this dominating uncertainty component of the spectral power responsivity calibration, a wavelength dependent correction was applied to the photometer spectral responsivity data. As a result of this correction, the 0.3 % to 0.6 % systematic errors decreased to 0.05 % for the overall visible range.

The measured aperture area was multiplied by the SCF measured spectral power responsivity of the photometer to obtain the SCF-based spectral irradiance responsivity. During the SCF calibrations, the wavelength shift of the monochromator was minimized to less than 0.1 nm before the spectral responsivity scans.

The SIRCUS and SCF measured spectral irradiance responsivities of the F100 photometer are shown in Fig. 10. The logarithmic scale shows that equal blocking was measured in both power and irradiance measurement modes.

The SCF-based spectral irradiance responsivity of both transfer standard photometers was compared to the SIRCUS measured spectral irradiance responsivity. The absolute difference for the trap-detector based photometer is shown in Fig. 11. The graph also shows the SCF determined spectral irradiance responsivity around the peak responsivity of the trap-photometer. The structures in the difference curve are caused by the filtered fringes of the SIRCUS data.

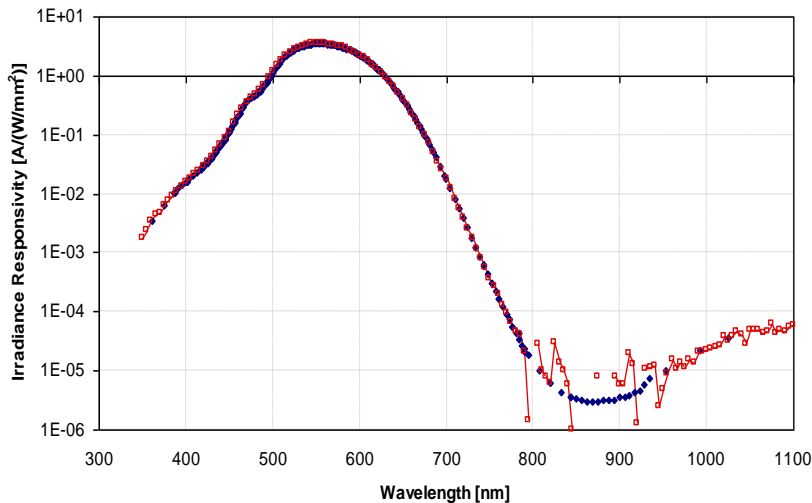


Fig. 10. SIRCUS (full diamond) and SCF (open square) measured spectral irradiance responsivities of the F100 photometer.

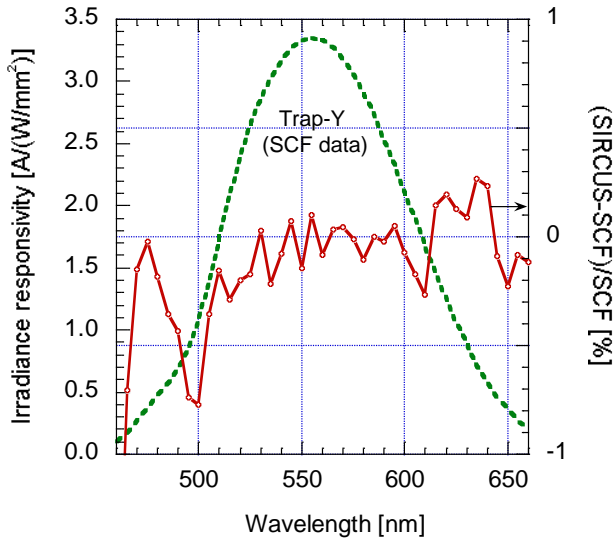


Fig. 11. Difference of the SIRCUS and SCF measured spectral irradiance responsivities of the trap-photometer.

The spatial uniformity of responsivity of the F100 photometer is shown in Fig. 12. The spatial scan was made at 555 nm with 0.5 mm increments. The diameter of the scanning spot was 1.1 mm. The 0.1 % contours illustrate the combined spatial non-uniformity of the illuminance measuring photometer including the transmittance changes of the photopic filter and the responsivity changes of the Si photodiode.

The current-to-voltage converters of the reference photometers were calibrated against the NIST reference current-to-voltage converter which has an uncertainty of 0.013 % ($k=2$) for all gain selections up to 10^{10} V/A [17]. This uncertainty is about six times smaller than the amplifier-gain calibration uncertainty at the SCF.

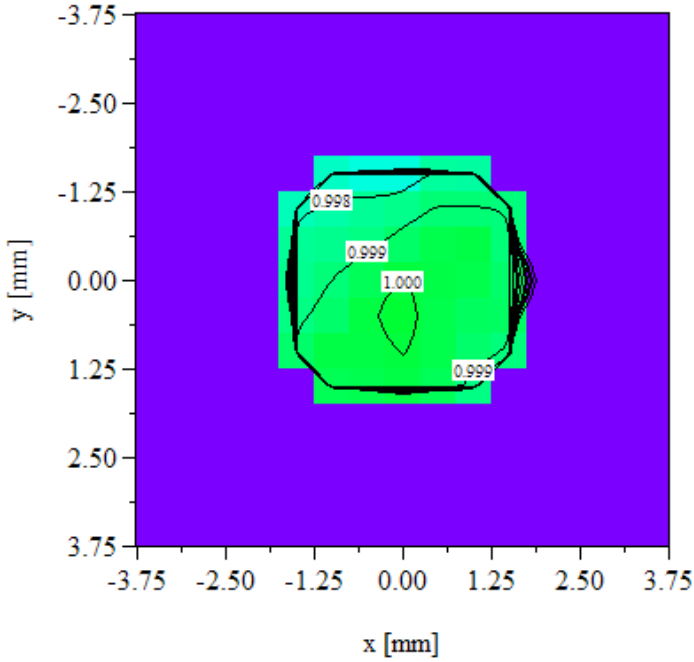


Fig. 12. Spatial non-uniformity of responsivity of the F100 photometer.

2.1.1.4. Illuminance responsivity

The illuminance responsivity (also called the absolute luminous responsivity) s , which is the ratio of the photometer output current to the illuminance measured by the photometer, was determined from the SIRCUS measured spectral irradiance responsivity $s_E(\lambda)$ and the incident irradiance $E(\lambda)$ from a CIE Standard Illuminant (Source) A source:

$$s = \frac{\int s_E(\lambda) E(\lambda) d\lambda}{K_m \int V(\lambda) E(\lambda) d\lambda} \quad (1)$$

where K_m is the maximum spectral luminous efficacy, 683 lm/W and λ is the wavelength.